IONIC MASS TRANSFER AND CONCENTRATION POLARIZATION AT ROTATING ELECTRODES

by

M. Eisenberg, C. W. Tobias and C. R. Wilke

Technical Report No. 3
Office of Naval Research
Contract No. Nonr 222(06)
Project No. NR. 359-270

October 15, 1953

Department of Chemistry and Chemical Engineering
University of California
Berkeley, California

TABLE OF CONTENTS

ABSTRACT

Rates of ionic mass transfer at nickel electrodes rotating about their axes in the center of stationary electrodes were studied using the ferri-ferrocyanide couple in alkaline solutions. A general mass transfer correlation was found to apply equally well to the dissolution rates of rotating solids and to the rates of ionic mass transfer at rotating electrodes. This correlation takes into account the physical properties of the system as well as geometric and hydrodynamic factors. The correlation enables the prediction of limiting currents and concentration polarization at rotating electrodes under a wide range of conditions.

The nature of the polarization involved in the reduction of $Fe(CN)_6^{-3}$ and the oxidation of $Fe(CN)_6^{-4}$ was also investigated. The polarization was found to depend strongly on the presence of "electrode poisons." With freshly prepared solutions, under exclusion of light and with cathodically treated nickel electrodes relatively small chemical polarizations were determined. For rotational speeds not exceeding Reynolds number 11,000, the chemical polarization was found to be negligible in comparison with the concentration polarization. Under such conditions the ferro-ferricyanide couple can be conveniently used to obtain mass transfer rates for various hydrodynamic conditions, or, conversely, to verify the validity of mass transfer equations by a comparison of experimental and calculated values of limiting currents and concentration polarization.

The rotating electrode model was found to be most suitable for studying the nature of electrolytic polarization phenomena on account of the uniformity of the current distribution as well as of the hydrodynamic diffusion layer at the electrode surface.

I. INTRODUCTION

The study of mass transfer at working electrodes has been found to be of fundamental importance (1, 2) in the analysis of electrode phenomena and in the consideration of concentration polarization, limiting currents and rates of electrode reactions. In recent years several typical cases have been analyzed by means of the methods of hydrodynamics and boundary layer theory, and for a few models experimental results were successfully correlated (1, 2). The effect of natural convection in electrolysis was quantitatively evaluated among others by Wagner (3) and Wilke et al. (4). The case of rotating disc electrodes was treated mathematically by Levich (5). This theory is applicable as long as the diffusion boundary layer at the disc is laminar. Along the lines suggested by Agar (6), Lin et al. (7) correlated limiting current densities for the inner electrode of an annular cell with streamline and turbulent longitudinal flow. An extension of this study for laminar and turbulent flow along flat plate electrodes was recently completed by Lin et al. (8).

The present investigation is concerned with cylindrical central electrodes rotating in concentric cylindrical cells. Among the many possible methods of stirring the case of a rotating electrode is most noteworthy not only because it affords experimental reproducibility, but also because it offers the application of methods of hydrodynamics and mass momentum transfer analogy in the interpretation and correlation of data (9, 10, 11). The theoretical analysis of this problem in case of electrodes is further facilitated by the uniformity of current distribution resulting from the geometry of concentric cylindrical electrodes

and the uniform thickness of the diffusion layer formed on the rotating electrode.

In recent years rotated electrode surfaces have found a number of applications in chemical analysis as well as in corrosion studies as a parallel tool to the polarographic methods (12, 13). Industrial applications of this forced convection model are known and further important uses are anticipated.

The effect of the speed of rotation upon the rate of mass transfer was first studied by Brunner (14, 15). He found that the diffusion layer thickness, δ, decreases with the 2/3 power of the speed. However, he considered neither the effect of rotor diameter or geometry nor the dependence on the physical properties of the electrolyte. Therefore only qualitative conclusions can be drawn from these experimental results.

Eucken (16) has analyzed the effect of laminar flow forced convection upon the rate of mass transfer at an electrode. In his experiments the external vessel containing the solution was rotated, and laminar flow past the fixed inner flat plate electrode resulted. Eucken's mathematical analysis is valid only for this particular condition. Kambara et al. (17) have adapted Eucken's treatment to the case of a 0.5 mm diameter platinum wire electrode projecting perpendicularly 6 mm from the axis of a rotating glass rod. In the derivation the assumption is made that the velocity gradient at the electrode surface is proportional to the rpm. This is valid in the case of Eucken's model, where laminar flow exists in the entire region of flow, but is inadmissible for the turbulent flow case, where laminar flow is restricted to the boundary layer adjacent to the electrode surface.

For the sake of clarity henceforth the term "rotating electrode" will be used only in reference to cylindrical electrodes rotating about their axis in the center of a stationary circular cylindrical electrode. Recently Raold and Beck (18) have used such rotating electrodes in a study of rates of dissolution of magnesium and its alloys in hydrochloric acid solutions. They found that the rates of dissolution increase in the region of low acid concentrations with the 0.71 power of the speed of rotation. At higher acid concentrations (1.4 molar and higher) the reaction rates become entirely independent of rotational speeds, as the stirring effect produced by the hydrogen bubbles evolving at the metal interface becomes predominant. This stirring effect, however, should not be ignored even at low acid concentrations because of turbulence caused by the hydrogen bubbles moving in the boundary layer adjacent to the dissolving magnesium rod. For this reason the work of Reald and Beck represents a rather special case of forced convection mass transfer.

The present work was undertaken with the following aims in mind:

(a) To establish correlations between the physical properties of a system, geometrical and hydrodynamic conditions, and the rates at which a solute (ion) is transferred to or from a rotating electrode.

(b) To determine whether such general mass transfer correlations enable the prediction of concentration polarization and limiting currents in steady state electrolysis.

II. EXPERIMENTAL

To assure the latter objective it was important to choose an electrode reaction which occurs with negligible chemical polarization. For such an electrode process the total measured polarization (ΔE_T) would represent concentration polarization (ΔE_{conc}) only, and would make a comparison between theoretical prediction and experiment possible. However, most of the known electrode reactions take place with considerable chemical polarization (ΔE_{chem}) when finite currents are passed. Some oxidation-reduction reactions have long been suggested by investigators (19, 20, 21) to occur with negligible chemical polarization. In a more recent study Moll (22) found no measurable chemical polarization for the ferrous-ferric couple at gold and platinum electrodes freshly treated by hydrogen and oxygen discharge. Essin and coworkers (23) made similar studies on the ferrocyanide-ferricyanide couple at platinum and nickel electrodes and concluded that there is no appreciable chemical polarization "when the metal is free of all film that may form on the surface." Carmody and Rohan (24) on the other hand have reported a measurable chemical polarization for this latter system on platinum. A similar conclusion was arrived at by Petrocelli and Paolucci (25) who studied this couple up to current densities of 25 mA/cm^2. They found, however, that "cathodic activation," i.e. a hydrogen discharge treatment of the electrode, tends to decrease chemical polarization.

For the purposes of this study smoothness of the electrode surface was important because of hydrodynamic considerations. In a redox electrolysis, unlike in a metal-deposition process, the electrode surface remains physically unaltered. Another advantage

of the redox reaction is that steady state electrode potentials are arrived at in much shorter time than in a deposition reaction.

These findings in addition to stability considerations of several contemplated couples resulted in the selection of the ferricyanide-ferrocyanide couple and nickel electrodes for the present studies. A large excess of sodium hydroxide was used in order to eliminate the contribution of ionic migration to the mass transfer (1).

Solutions of potassium ferri- and ferrocyanide and particularly the ferrocyanide, are known to decompose slowly by the action of light resulting in the formation of cyanide and hydroxide ions according to the following equations (26, 27):

$$[Fe(CN)_6]^{-4} + H_2O \underset{\text{dark}}{\overset{\text{light}}{\rightleftharpoons}} [Fe(CN)_5]^{-3} + CN^-$$

$$CN^- + H_2O \rightleftharpoons HCN + OH^-$$

In alkaline solutions kept in darkness the decomposition of these cyanide complexes is practically eliminated (28). Solutions used in these studies were freshly prepared for each series of runs in black Jena glass bottles.

A. Apparatus and Procedure

A concentric cylindrical cell, 6.16 inches high, built from acrylic plastic (lucite) was equipped with grooved endplates which could hold as desired one of the three cylindrical plastic tubes of internal diameter 2.46, 4.00 and 5.47 inches. (See Figures 1 and 2.) A ½-inch diameter stainless steel driving shaft passed through a teflon packing gland through the top plate and was equipped with a 1/4-inch standard thread allowing the nickel electrodes of various diameters (1.273, 2.46 and 5.024 cm) to be screwed onto it. The rotated electrode was supported from the

bottom by a guide pin and teflon lining in order to eliminate eccentric motion. The concentric outer cylindrical nickel electrodes (of inside diameter 6.07, 9.87 and 13.69 cm), all 15.11 cm long, were fitted tightly into the corresponding lucite tubes. (See Figures 1 and 2). The cell was made liquid tight with neoprene rubber gaskets placed into the grooves. A ground glass joint thermometer fitted into the top plate with its bulb reaching about 3/4 in. into the cell interior. The entire assembled cell with supporting structure designed to eliminate vibrations is shown in Figure 3.

The electrodes permitted a variation of the ratio of gap to the diameter of the inner electrode (h/d_1) ranging from 0.104 to 4.88. A lucite nipple on the top plate of the assembled cell was screwed into a small tapered hole which on the inside of this plate ended with a 1/4 mm diameter and was located at a distance of 2.541 cm from the axis of the cell. (Figure 4.) Through this hole and a piece of polyethylene tubing a continuous liquid junction led to reference cell No. 1 equipped with a nickel electrode and filled with the same solution as that in the electrolytic cell. Reference cell No. 2 was connected with the cell by means of a teflon nipple leading through the center of the lucite cylinder and ending flush with the inner side of the outside electrode with a 1/4 mm hole. Such arrangements of the liquid junction leading to the reference electrodes are preferable for two reasons: (a) the flow pattern in the cell remains undisturbed; and (b) a distortion of the current distribution over the electrode surface is avoided.

As can be seen from the diagram in Figure 4, a potential

measurement of the rotating electrode by means of the reference electrode No. 1 involved an ohmic potential drop over the annular solution space between the radius r_i of the rotating electrode and the distance of 2.54 cm at which the small opening leading to that reference cell was located. For a total current, i, this ohmic drop was therefore

$$iR_{(1)} = \frac{i}{2\pi K h'} \ln \frac{2.54}{r_i} \qquad \text{(Ia)}$$

where R = resistance, ohms.

r_i = radius of rotated inner electrode used, cm.

h' = height of the cell, here 15.11 cm.

K = conductivity of the solution, $ohm^{-1}cm^{-1}$.

Similarly a potential measurement of the rotated electrode by means of the reference No. 2 involved an ohmic drop given by:

$$iR_{(2)} = \frac{i}{2\pi K h'} \ln \frac{r_o}{r_i} \qquad \text{(Ib)}$$

Since r_o, the internal radius of the outer electrode, was either 6.84 cm (Series I of runs), 4.94 cm (Series II of runs) or 3.035 cm (Series III of runs), the ohmic drop could be computed more reliably by equation Ib, i.e. using reference No. 2. This is particularly true as a small geometrical misalignment will cause a lesser relative error in the ratio r_o/r_i of equation Ib.

In all runs potential measurements of the rotating electrode were taken by means of both reference junctions selected one at a time with switch S-1 (Figure 4). The net values obtained after subtracting $iR_{(1)}$ and $iR_{(2)}$ drops respectively rarely differed by more than 1%. However, for reasons stated above, in most cases measurements with reference electrode No. 2 were preferred over an arithmetic average of the two measurements.

The electrical connection to the rotating electrode was accomplished by means of a mercury well (W in Figure 4). A copper contact screw provided the connection to the outer stationary electrode. The current was measured with a D.C. milliammeter[1] or a D.C. ammeter.[2] All ammeters were carefully calibrated by means of standard resistors. Selector switch S-2 (Figure 4) permitted measurements of the potential by either of the following instruments:

a. Recording potentiometer[3] with five ranges, the largest being up to 500 mV.

b. Manual potentiometer,[4] using a high sensitivity galvanometer as a zero instrument.[5]

The recorder was usually used first to ascertain that a steady state polarization was achieved and then the final value was measured accurately by means of the manual potentiometer.

Sodium hydroxide, 2 N, was used as neutral electrolyte in the preparation of five approximately equimolar potassium ferricyanide and potassium ferrocyanide solutions in the concentration range of 0.009 to 0.204 mols per liter. C.P. reagents[6] were used throughout. These solutions were prepared freshly prior to use and kept in black Jena glass bottles to minimize the effects of light (see previous discussion). Slight changes in concentrations of ferri- and ferrocyanide ions caused by use of a solution up to limiting

---

[1] Weston (Model 45).
[2] Cenco (Model 6935).
[3] Minneapolis Honeywell Co. (Model Y-153-X-12).
[4] Leeds and Northrup, type K-2 (Model No. 7552).
[5] Leeds and Northrup (No. 2430).
[6] Merck and Co.

current densities were followed up by a strict analytical control. Ferricyanide was determined by the iodometric procedure (29) and the ferrocyanide by permanganate titration (30).

Before introducing into the cell each solution was alternately de-aerated in a glass column by means of vacuum and saturated with nitrogen several times to remove the dissolved oxygen. The presence of a considerable amount of dissolved oxygen in the cell would have interfered with the electrode reactions of the ferricyanide and ferrocyanide, particularly at low concentrations. Furthermore it was felt that in absence of oxygen the nickel electrodes would remain longer in an "active" state.

Prior to each assembling of the cell the smooth electrodes were polished with rouge paper, washed with CCl_4 and treated cathodically in a 5% NaOH solution at a current density of 20 mA/cm^2 for 12-15 minutes.

The assembled cell was filled with a given solution at approximately 25°C, the inner electrode set into rotation at a selected speed. The value of the electrode potential at no current flow (ZCP) was measured with both references. These were later subtracted (with proper sign) from the "at current" values. Thus any "static" potential differences due to differences in surface structure of the electrodes could be accounted for. A relatively small current was then applied and the potential of the rotating electrode followed up by means of one of the two reference electrodes and the recording potentiometer until steady state was achieved. The final values were then measured with the manual potentiometer using both reference electrodes consecutively. Steady state polarization was obtained within a

few seconds at high speeds and within 2 to 3 minutes at low speeds. Achievement of the steady state, while not essential for the determination of limiting currents, was important for the subsequent calculations of chemical polarization. A reliable comparison of the concentration and chemical polarization can be made only under steady state conditions. Current was increased in small increments until the limiting current, noted by a sudden rise in potential, was attained. At a given speed each run was first completed with the rotor as the cathode. Then the polarity was reversed and a run was carried out with the rotor as the anode. When a series of runs with speeds ranging from 30 to 1650 rpm was complete the cell was taken apart, the electrodes treated, as described previously, and reassembled with another electrode diameter but with the same inner electrode. Thus the effect of the gap between the concentric cylindrical electrodes was studied for a given solution, given diameter of the rotating electrode and given angular velocity. The temperature of 25°C $\pm$ 0.3 was maintained by blowing preheated or precooled air on the outside of the cell. Physical properties required for correlative study were determined for each of the solutions within the temperature range 20-30° C.

Conductivities were measured in a conventional conductivity cell, calibrated with a 0.9996 molar KCl solution, using an audio-oscillator[1] as a power source for 1000 cycle A.C., a Wheatstone bridge and an oscilloscope[2] as a zero instrument.

Viscosities of the solutions relative to water were measured at several temperatures in a thermostat with an Ubbelohde pipette,

---

[1] Hewlett-Packard Model 200 C.

[2] RCA No. 155A.

and the absolute viscosities calculated using densities obtained by picknometer determinations.

Diffusion coefficients for the ferri-ferrocyanide ions were measured by means of the capillary method (31).

B. Methods of Calculation

1. Ionic Mass Transfer

The potential values obtained for each run were first corrected by subtracting (with proper sign) the zero current potential (ZCP) differences and the corresponding iR drops calculated by means of equation I. These net resulting values represented the total polarization, ΔE_T. From the known areas of the rotating electrodes the current densities were calculated and plots of current density, I (mA/cm^2) versus total polarization, ΔE_T (mV) were prepared. The limiting current densities were then determined for each run at the plateau of the curve, i.e. as the value at which a small increment of current caused a sudden rise of potential. At this point in case of cathodic ferricyanide reduction runs, the consecutive electrode process was hydrogen evolution. This, however, did not take place before the potentials exceeded 600-700 mV. For anodic oxidation of ferrocyanide the plateau was shorter as the consecutive reaction (i.e. oxygen evolution) took place at ΔE_T values of 200-250 mV. As illustrations Figures 5 and 6 show sets of cathodic and corresponding anodic runs for solution No. 9 at speeds up to 1650 rpm. The limiting cathodic current densities (I_c) and the limiting anodic current densities (I_a) are given in the corresponding figures.

At limiting current when the interfacial concentration of the reacting species becomes zero, the rate of ionic mass transfer of

ferricyanide ion to the cathode or of ferrocyanide ion to the anode can be expressed as (1):

$$N = \frac{I_L}{nF}(1 - t_i) = k_L c_o \qquad (II)$$

where I_L = cathodic (I_c) or anodic (I_a) limiting current densities, amps/cm².

n = valence charge of reacting ion.

F = the Faraday constant.

c_o = bulk concentration of reacting ion, moles/cc.

t_i = transference number of the reacting ion.

k_L = average mass transfer coefficient, cm/sec.

Since the estimated transference numbers of ferri- and ferrocyanide ions did not exceed 0.03 (and was usually much lower) due to the large excess of NaOH used as the indifferent electrolyte, equation II can be rewritten as:

$$N = \frac{I_L}{nF} = k_L c_o \qquad (IIa)$$

Thus by means of equation IIa the average mass transfer coefficient, k_c, for the ferricyanide reduction, and k_a for ferrocyanide oxidation were calculated for each run.

From the measured values of viscosity, μ, density, ρ, and diffusion coefficients, D_{ferri} and D_{ferro} corrected to the temperature of the given runs, the corresponding Schmidt groups $Sc = \mu/\rho D$ were computed for the anodic and cathodic experiments.

The Reynolds number, characterizing the flow produced in the cell, was found by the authors (see reference 32) to involve the diameter of the rotating electrode as the characteristic length dimension and not the gap between the cylindrical electrodes.

Accordingly the Reynolds number was computed as:

$$R_d = \frac{V \cdot d_i}{\nu} \qquad \text{(III)}$$

where V = peripheral velocity - cm/sec.

d_i = diameter of rotating electrode, cm.

ν = kinematic viscosity, cm^2/sec.

2. Concentration Polarization and Chemical Polarization

It is clear that as far as mass transfer studies are concerned, it is not necessary for the electrode reaction to take place with negligible chemical polarization. The mass transfer coefficient, k_L, could be calculated for any current density if in addition to the bulk concentration, c_o, the interfacial concentration, c_i, was known. Since an accurate experimental determination of c_i is extremely difficult, mass transfer coefficients are most conveniently obtained from limiting current measurements, as outlined in the preceding section.

However, an electrode reaction with negligible chemical polarization was desirable in these studies in order to ascertain experimentally whether correct predictions of limiting currents and concentration polarization can be made from a general mass transfer correlation for rotating cylinders.

The ferri-ferrocyanide couple was therefore investigated as to the nature of the polarization associated with both the cathodic reduction of ferricyanide and the anodic oxidation of ferrocyanide on nickel electrodes. This was done as follows:

a. From graphs of current density, I, versus total polarization, ΔE_T (of the type shown in Figures 6 and 7), pairs of values of I and ΔE_T were read off at equal current density increments and tabulated up to current densities equal to 70-75% of the limiting current density.

b. Using the cathodic limiting current, I_c, and the anodic limiting current, I_a, (both obtained for the same solution, cell geometry and speed), the concentration polarization, ΔE_{conc}, for this redox couple was calculated (23, 33) for each current density, I, by means of the following equations:

$$\Delta E_{conc.} = \frac{RT}{nF} \ln \frac{1-I/I_c}{1+I/I_a} \quad \text{(for cathodic case)} \tag{IVa}$$

$$\Delta E_{conc.} = \frac{RT}{nF} \ln \frac{1+I/I_c}{1-I/I_a} \quad \text{(for anodic case)} \tag{IVb}$$

c. Chemical polarization ($\Delta E_{chem.}$) at each of the applied current densities, I, was calculated by subtracting the calculated $\Delta E_{conc.}$ from the experimentally obtained total polarization, ΔE_T, i.e.,

$$\Delta E_{chem.} = \Delta E_T - \Delta E_{conc.} \tag{V}$$

It is interesting to note that from equations (IV) and (V) for the case of a redox electrode reaction with negligible chemical polarization a plot of the experimental values of ΔE_T versus log Q, where

$$Q = \frac{1 \mp I/I_c}{1 \pm I/I_a} \tag{VI}$$

(upper sign for cathodic case, lower for anodic case)

should yield a straight line with the slope $2.303 \frac{RT}{nF}$. For the ferri-ferrocyanide couple n = 1 and expressing potentials in millivolts (mV) the slope for experiments performed at 25° C should be 59.1.

---

[1] Actually the derivation of this equation assumes that the mass transfer coefficient is independent of the current density. In forced convection such an assumption is well justified.

III. RESULTS AND DISCUSSION

A. Correlation of Mass Transfer Rates

The ionic mass transfer results here presented were part of a broader study involving dissolution of rotating cylinders cast from Benzoic and Cinnamic acid into water and aqueous glycerol solutions (32). A general type of correlation based on the methods of the momentum-mass transfer analogy was obtained using the following parameter:

$$j_D' = \frac{k}{V} (Sc)^{0.644} \qquad \text{(VII)}$$

in which the Schmidt number $Sc = \frac{\nu}{D}$ accounts for the physical properties of the system and k_L is given by equation Ia.

Figures 7 and 8 show logarithmic j_D' vs. R_d plots of the mass transfer data for the reduction of ferricyanide and oxidation of ferrocyanide respectively. Table 1 gives a typical set of data,[1] including the physical properties, for one of the five solutions studied. Average deviations of the points in Figures 7 and 8 from the best line are ± 7% and ± 6.6% for the two electrode reactions. These experiments involved a Schmidt number variation of 2230 to 3650 and a Reynolds number range of 112.0-162,000 (peripheral velocities 1.17 to 426 cm/sec). Limiting current densities varied from 0.43 to 113 mA/cm^2.

In Figure 9 the lines correlating the electrolytic data are compared with result. obtained by solid dissolution studies. The results for the various systems agree with each other within 7% and lie all within the experimental errors involved in the

---

[1] Complete data are given in Technical Report No. 2, Nonr 222(06), September 15, 1953 ("Mass Transfer at Rotating Cylinders," by M. Eisenberg, C. W. Tobias and C. R. Wilke).

determination of the frictional drag coefficient f/2 obtained by Theodorsen and Regier (11).

Such an agreement is very encouraging in view of the Chilton-Colburn analogy (34) which suggests that

$$j_D = \frac{k_L}{V} \phi\ (Sc) = f/2 \qquad \text{(VIII)}$$

where ϕ (Sc) represents a function of the Schmidt number. (For a detailed discussion see ref. 32.)

In Figure 10 all mass transfer data for three solid dissolution systems and the two electrolytic redox reactions were all plotted together. The best curve (within $\pm$ 8.3%) through all points is represented by the coordinates given in Table 2.

In the Reynolds number range 1000-100,000 the data are best represented by a straight line (dashed in Figure 10) given by the equation

$$j_D' = \frac{k}{V} Sc^{0.644} = 0.0791\ R_d^{-0.30} \qquad \text{(IX)}$$

From equation (IX) a number of interesting practical relations may be derived.

Recalling that the mass transfer coefficient $k = I_L/nFc_o$, the following relations for the limiting current density may be obtained:

$$I_L = 0.0791\ nFc_o\ V\left(\frac{Vd_i}{\nu}\right)^{0.30}\left(\frac{\nu}{D}\right)^{0.644}$$

$$= 0.0791\ nFc_o\ V^{0.70}\ d_i^{-0.30}\ \nu^{-0.344}\ D^{0.644}$$

$$= nF\ \frac{Dc_o}{\delta} (amps/cm^2) \qquad \text{(X)}$$

The diffusion layer thickness, δ, in cm., is then given by:

$$\delta = \frac{1}{0.0791\ V^{0.70}\ d_i^{-0.30}\ \nu^{-0.344}\ D^{-0.356}}$$

$$= 12.64 \times \frac{d_i^{0.30}\ \nu^{0.344}\ D^{0.356}}{V^{0.70}}$$

$$= 99.62\ \frac{d_i^{-0.40}\ \nu^{0.344}\ D^{0.356}}{S^{0.70}} \qquad \text{(XI)}$$

where ν = kinematic viscosity, $cm^2/sec.$

D = diffusion coefficient, $cm^2/sec.$

S = rotational speed, rpm.

$V = \frac{\pi}{60} w\ d_i$ = peripheral speed, cm/sec.

d_i = rotor diameter, cm.

Thus the diffusion layer thickness δ depends not only on the rotational speed, but also on the rotor diameter as well as on the physical properties of the system such as viscosity and diffusivity. The latter three variables were not considered by Brunner(14).

With the assumption that δ is independent of the rate (i.e. of the current density), as was suggested by Agar (6), one can write:

$$\frac{I}{nF} = \frac{D}{\delta}(c_o - c_i) \qquad \text{(XIIa)}$$

where c_o and c_i denote the bulk and interfacial concentrations respectively.

Hence for a given applied c.d., I, the concentration of the reacting ion at the electrode interface c_i may be calculated by means of the relation:

$$c_i = c_o - \frac{I}{nFD}\delta \qquad \text{(XIIb)}$$

The thickness of the diffusion layer, δ, is obtained for a given geometry, speed and physical properties of the electrolyte by means of equation (XI).

Previous studies relating to mass transfer at rotating electrodes were limited in scope and can be compared to the present work only in respect to the functional dependence on the rotational speed. Reald and Beck (18) found for rotating magnesium electrodes:

$$k_L = \text{const.}\ v^{0.7} \qquad \text{(XIII)}$$

This is in agreement with the results of the present study since equation (XIII) can be shown to follow from equation (V) for a given system (constant ν and Sc) and given rotor diameter. The experiments of Brunner (14) involved rather impractical geometries and poorly defined experimental conditions. His results may be expressed in the form:

$$k_L = \text{const.}\ (\text{rpm})^{2/3} \qquad \text{(XIV)}$$

For a given rotor diameter and given set of physical properties of the system this relation is in approximate agreement with the results of the present study.

B. Limiting Currents and Concentration Polarization

1. The Nature of Polarization of a Redox Electrode

For the total polarization, ΔE_T, of a redox electrode Petrocelli (32) obtained a general equation[1] which in a somewhat modified form may be written as:

$$\Delta E_T = \frac{RT}{nF} \ln \left[\frac{1 - I/I_c}{I + I/I_a} - \frac{I \frac{I_a}{I_o}}{(I_a + I)\ \exp(-\alpha \Delta E_T \frac{nF}{RT})} \right] \qquad \text{(XV)}$$

[1] Analogous relations have recently been obtained by a number of investigators (35, 36).

where I_c and I_a = absolute values of cathodic and anodic limiting current densities respectively.

I = applied current density (positive for cathodic, negative for anodic case).

α = a constant between 0 and 1 (usually close to 0.5) representing the portion of the electrical potential difference across the activation energy barrier, which acts in the cathodic direction.

i_o = exchange current density, representing the rate of forward (cathodic) and also backward (anodic) reaction at the reversible, i.e. open, circuit potential.

Using the concepts of the absolute reaction rate theory (37) it is possible to show (32) that the exchange current density

$$i_o = \frac{nF}{N} \frac{kT}{h} c_o \cdot e^{\frac{-\Delta F^*}{RT}} \qquad \text{(XVI)}$$

where ΔF^* = standard free energy change of the activation process (i.e. at open circuit), ergs/mole.

N = Avogadro number, 6.023×10^{23}, molecules/mole.

h = Planck constant, 6.624×10^{-27}, erg-sec/molecule.

k = Boltzmann constant, 1.3805×10^{-6}, erg/°K-molecule.

c_o = bulk concentration of the reacting ion, moles/L.

n, F, R and T have the usual meaning.

Thus, at constant T, i_o depends only on the activation energy ΔF^* and the bulk concentration, c_o, of the reacting ions. For a given electrode reaction the activation energy can be assumed to be constant provided that "electrode poisons" are absent (22, 35). Under such conditions the exchange current density, i_o, depends only upon the concentration, c_o.

In equation (XV) the first term in the bracket represents the contribution of the concentration polarization, and the second represents the chemical polarization. The relative magnitude of this second term depends primarily on I_a/i_o, the ratio of the limiting c.d. to the exchange c.d.

For a given electrode system the limiting c.d., I_a, increases with the 0.70 power of the rotational velocity, according to equation (X); i_o, however, remains unaffected. Hence at high rotational speeds, i.e. large values of I_a/i_o, the chemical polarization should become significant in comparison with the concentration polarization. It is obvious, therefore, that in order to ascertain experimentally whether a given electrolytic redox reaction comes close to thermodynamic reversibility, i.e. takes place with a comparatively small chemical polarization, ΔE_T vs. I curves must be obtained at high rotational speeds. From such curves (see for example Figures 5 and 6) plots of the total polarization, ΔE_T against $\log \frac{1 \mp I/I_c}{1 \mp I/I_a}$ can be prepared as described previously. A comparison of equations (IV) and (XV) shows that if chemical polarization is negligible, i.e. $\Delta E_T \approx \Delta E_{conc.}$, the experimental points in such plots should fall close to a straight line with a slope of 59.1 (at 25° C, expressing polarization in mV). This type of plot is very convenient as the distance of a given point from the straight line with the slope 59.1 gives directly the value of the chemical polarization and demonstrates the importance of the latter relative to the concentration polarization (see for instance in Figure 13).

Tables 3-7 give typical sets of results for several ferri-ferrocyanide solutions. The values of $\Delta E_{conc.}$ and $\Delta E_{chem.}$ were

calculated according to equations (IV) and (V). Data for three experimental series were plotted in Figure 11. The solutions used were only 0.05 m. and 0.01 m. in ferri- or ferrocyanide, hence according to equations (XV) and (XVI) some chemical polarization may be expected. However, as Figure 11 shows, even up to peripheral velocities of 157.3 cm/sec the total polarization, ΔE_T, consists almost entirely, within limits of experimental accuracy, of concentration polarization.

The predominant importance of the stirring rate as represented by the peripheral velocity, V, is interestingly demonstrated in Figure 12 for a solution of a relatively high concentration (number 9, approximately 0.20 of $Fe(CN)_6^{-3}$ and $Fe(CN)_6^{-4}$). For runs up to a velocity V = 115 cm/sec the data fall close to the straight line with a slope 59.1, the value for the so-called reversible electrode. At higher speeds, i.e. when the ratio I_a/i_o increases, chemical polarization becomes relatively significant. For instance at V = 333 cm/sec, when the concentration polarization is 59.1 mV, the corresponding chemical polarization has already reached 18.4 mV (Figure 12). Hence, in case of a reaction where I_a/i_o is not very small, it is possible to increase this ratio by increasing I_a with stirring (rotational speed). In this way a reaction in which the polarization is predominantly controlled by mass transfer (i.e. concentration polarization) may be converted to one which is under activation control, involving large chemical polarization.

As shown previously the exchange current density, i_o, depends greatly on the activation energy ΔF^* necessary for the reaction to proceed. The latter has been found by many investi-

gators to increase in the presence of electrolytic poisons (22, 35). Thus, according to equation (XVI) the exchange c.d., i_o, may be expected to decrease significantly under such conditions. Indeed, in a special study on the effects of the better known electrode poisons Gerischer (35) found, for instance, that at platinum electrodes treated with a 2×10^{-5} m. H_2S solution for one minute and 60 minutes respectively, the exchange c.d., i_o, for the Fe^{+3}/Fe^{+2} couple dropped to 10.8% and 1.7% of the original (active state) value, respectively. The highly alkaline solutions used in the present studies, when exposed to air, could dissolve an amount of H_2S sufficient to decrease i_o and consequently increase the chemical polarization. The effects of other electrode poisons should, of course, be taken into account as well. For instance, HCN formed through the photochemical decomposition of ferrocyanide may be expected to exercise a powerful effect. Several investigators (38, 21) have also concluded that even electrodes made of "noble" metals such as gold, silver and nickel become gradually covered with oxide films (when used in air-saturated solutions) causing a large increase in polarization.

In a special study designed to demonstrate the effect of electrode poisons, ΔE_T - I data were obtained for an alkaline ferro-ferricyanide solution, which was exposed to air and light for several days. The nickel electrodes, used in this study, were cleaned in the same manner as described previously, but were not given any cathodic hydrogen discharge treatment. Figure 13 shows the results for solution No. 1 in the form of ΔE_T vs. log Q plot. Large chemical polarizations (demonstrated by the deviations from the $\Delta E_{conc.}$-line) were obtained in spite of the relatively low

rotational speeds (up to V = 56.6 cm/sec). The values of $\Delta E_{conc.}$ = -59.1 mV and $\Delta E_{chem.}$ = -47.9 mV (hence ΔE_T = -107 mV) indicated in Figure 13 (cathodic case) are for an applied c.d. of 12.1 mA/cm^2 and a peripheral speed of 24.6 cm/sec. It is interesting to compare these with a freshly prepared solution (number 9) at about the same c.d. and rotational speed.[1] Thus at a c.d. I = 12 mA/cm^2 and V = 20 cm/sec a total cathodic polarization (ΔE_T) of only -43. -43.5 mV was measured for solution number 9 (see Table 6). The corresponding concentration polarization was calculated to be -47.1 mV.[2] Hence no measurable chemical polarization was determined in this case, while at the same c.d. in the case of the "poisoned" electrode, $\Delta E_{chem.}$ represented about 45% of the total electrode polarization.

With regard to the ferro-ferricyanide couple the following conclusions may be drawn on the basis of the present study.

(a) Only freshly prepared and de-aerated alkaline potassium ferri- and ferrocyanide solutions should be used with a maximum possible exclusion of light. The electrode (platinum or nickel) should be given a cathodic hydrogen treatment prior to each experiment.

---

[1]The difference in concentrations of the reacting ions between solutions number 1 and 9 (a factor of two) does not significantly affect this comparison, primarily because the ratio I_a/i_o is independent of the bulk concentration of the reacting ion.

[2]Actually the absolute value of the total polarization, ΔE_T, cannot be smaller than that of concentration polarization $\Delta E_{conc.}$ Whenever this seems to be the case, it must be attributed not only to experimental inaccuracies but partly also to the possibility that the achievement of a steady state polarization of the electrode was not quite complete. Fortunately in no case were these deviations very serious.

(b) With the above precaution a reasonably small chemical polarization, $\Delta E_{chem.}$, is associated with the electrolytic redox reaction. The amount of $\Delta E_{chem.}$ involved depends on the magnitude of the I_a/i_o ratio, i.e. on the rate of stirring (on which the limiting c.d., I_a, depends). For rotating electrodes up to a peripheral velocity of V = 115 cm/sec the electrode reaction is predominantly mass transfer controlled and the chemical polarization is negligibly small. The above peripheral velocity corresponds to a Reynolds number of 11,000. It should be reasonable to assume that in many other types of flow up to R_d = 11,000 a negligible $\Delta E_{chem.}$ may be expected for the ferri-ferrocyanide couple.

(c) Under conditions (see above) at which the total electrode polarization is almost entirely represented by concentration polarization, the general mass transfer correlation for rotating cylinders (equation VII) can be used to predict the diffusion layer thickness, δ, the limiting current density, I_c or I_a, and the concentration polarization, $\Delta E_{conc.}$ (see equations X, XI and IV). Conversely from a given measured polarization the interfacial concentration, c_i, of the reacting ion may be calculated at an applied current density.

To illustrate the latter point, calculations of δ, I_c, I_a, and $\Delta E_{conc.}$ have been carried out below for a rotating electrode in an alkaline potassium ferro-ferricyanide solution. To facilitate a comparison with experimental measurements the physical data for one of the systems studied were used.

2. Illustrative Example

Assumed Solution: (Equivalent to Solution No. 9)
0.1976 m $K_3Fe(CN)_6$
0.2027 m $K_4Fe(CN)_6$
2.004 m NaOH

Data:

Electrode diameter, $d_1 = 1.273$ cm

Rotational speed, S = 300 rpm

Peripheral Velocity, $V = \frac{S}{60} \pi d_1 = \frac{300}{60} \times 3.1416 \times 1.273$

$= 20.0$ cm/sec

Reynolds number, $R_d = 1,789$

Temperature, 25° C

Kinematic viscosity, $\nu = 1.423 \times 10^{-2}$ cm²/sec

Diffusion coefficient of $Fe(CN)^{-3}$, $D_{ferri} = 0.454 \times 10^{-5}$ cm²/sec

Diffusion coefficient of $Fe(CN)^{-4}$, $D_{ferro} = 0.390 \times 10^{-5}$ cm²/sec

Concentration of $Fe(CN)^{-3}$, $c_{ferri} = 0.1976 \times 10^{-3}$ moles/cc

Concentration of $Fe(CN)^{-4}$, $c_{ferro} = 0.2027 \times 10^{-3}$ moles/cc

Diffusion Layer Thickness, δ

From equation (XI):

$$\delta_{(cm)} = 12.64\ d_1^{0.30}\ V^{-0.70}\ \nu^{0.344}\ D^{0.356}$$

Hence for the cathodic case:

$$\delta_{ferri} = 12.64\ (1.273)^{0.30}(20.0)^{-0.70}(1.423)^{0.344}(0.454 \times 10^{-5})^{0.356}$$

$$= 4.840 \times 10^{-3} \text{ cm}$$

$$\delta_{ferro} = 12.64\ (1.273)^{0.30}(20.0)^{-0.70}(1.423)^{0.344}(0.390 \times 10^{-5})^{0.356}$$

$$= 4.585 \times 10^{-3} \text{ cm}$$

Limiting Current Densities

Cathodic limiting c.d.,

$$I_c = \frac{nFD}{\delta} c_{ferri} \frac{1 \times 96,500 \times (0.453 \times 10^{-5})}{4.840 \times 10^{-3}} \times (0.1976 \times 10^{-3})$$

$$= 17.89 \times 10^{-3} \text{ amps/cm}^2 = 17.89 \text{ mA/cm}^2$$

as compared to experimentally determined

$$I_c = 16.6 \text{ mA/cm}^2$$

$$\text{Deviation} = 7.6\%$$

Anodic limiting c.d.,

$$I_a = \frac{nFD}{\delta_{ferro}} c_{ferro} = \frac{1 \times 96{,}500 \times (0.390 \times 10^{-5})}{4.585 \times 10^{-3}} \times (0.2027 \times 10^{-3})$$

$$= 16.64 \times 10^{-3} \text{ amps/cm}^2 = 16.64 \text{ mA/cm}^2$$

as compared to experimentally determined

$$I_a = 16.4 \text{ mA/cm}^2$$

$$\text{Deviation} = 1.5\%$$

<u>Concentration Polarization at Applied c.d., I = 10 mA/cm²</u>

$$\text{Cathodic } \Delta E_{conc.} = 59.1 \log \frac{1 - I/I_c}{1 + I/I_a} = 59.1 \log \frac{1-10/17.89}{1+10/16.64}$$

$$= -33.1 \text{ mV}$$

as compared to the experimentally measured total cathodic polarization

$$\Delta E_T = -33.0 \text{ mV}$$

$$\text{Anodic } \Delta E_{conc.} = 59.1 \log \frac{1 + I/I_c}{1 - I/I_a} = 59.1 \log \frac{1+10/17.89}{1-10/16.64}$$

$$= +34.9 \text{ mV}$$

as compared to the experimentally measured total anodic polarization

$$\Delta E_T = 32.8 \text{ mV}$$

Hence chemical polarization is negligible for these cathodic and anodic runs, and prediction of the total polarization ΔE_T is possible. It should be noted that the general mass transfer

correlation enables the prediction of limiting currents and concentration polarization even when the chemical polarization is large; however, then the total electrode polarization could not be calculated.

The ferro-ferricyanide couple can thus be used conveniently to study mass transfer in liquids for various types of geometries and hydrodynamic conditions. The advantages of using an electrolytic redox reaction over solid dissolution for purposes of studying rates of mass transfer are:

(a) Achievement of steady state in a relatively short time.

(b) Direct control of rates, i.e. applied current. (This is not possible in case of solids.)

(c) Preservation of the smooth interfacial surface throughout the experiment.

(d) Higher accuracy and convenience in determination of the rates of mass transfer.

The present study has proven that, when properly carried out, the ferro-ferricyanide electrode reactions may be considered to remain predominantly under mass transfer control up to stirring rates corresponding to $R_d = 11{,}000$. However, the chemical polarization is essentially present whenever finite currents are passed, and becomes significant at high stirring rates. The reason Essin and co-workers (23) could claim that the electrolytic reactions of the ferri-ferrocyanide couple involve only concentration polarization is that their experiments were carried out at low stirring rates.

Under proper experimental conditions, when the concentration polarization is accounted for, the ferri-ferrocyanide couple is

not far from thermodynamic equilibrium, i.e. the activation energy ΔF^* is not very large. For the electro-chemical reaction which takes place at the electrode interface itself Lewartowicz (36) discussed two rate-determining steps. One step involves the electron transfer at the interface of the electrode, the other the change in the hydration of the ion undergoing the recharge. For the ferri-ferrocyanide couple this may be expressed as:

$$Fe(CN)_6^{-3}(H_2O)_m + e^- \rightleftharpoons Fe(CN)_6^{-4}(H_2O)_n + (m-n)H_2O$$

Numerous investigators (39, 40, 41) have found that an ion is more hydrated the larger its charge and the smaller its radius. Hence the activation energy of the total process is composed of the energy necessary for the electron passage between the ion and electrode and of the hydration energy. The latter depends only on the state of hydration of the oxidized and reduced ions but the former is probably the one which is affected by the presence of electrolytic poisons adsorbed at the electrode surface. Lewartowicz's experiments (36) on Fe^{+3}/Fe^{+2}, Ce^{+4}/Ce^{+3} and quinone/hydroquinone couples have shown a small chemical polarization to be involved in each case. His results support in a general sense the above discussed mechanism of the electrolytic redox reaction.

It seems reasonable that electrode reactions involving only electron transfer and change in the degree of ion hydration would involve small activation energies, compared to reactions involving the breaking or formation of chemical bonds.

LITERATURE CITED

1. Eisenberg, M. Studies on the Role of Ionic Diffusion and Mass Transfer in Electrode Processes, M.S. Thesis, University of California, Berkeley (1951).

2. Tobias, C. W., Eisenberg, M., and Wilke, C. R. J. Electrochem. Soc. 99, 359c (1952).

3. Wagner, C. J. Electrochem. Soc. 95, 161 (1949).

4. Wilke, C. R., Eisenberg, M., and Tobias, C. W., J. Electrochem 100, 513 (1953).

5. Levich, B. Acta Physicochimica (U.S.S.R.) 17, 257 (1942).

6. Agar, J. N. Disc. Faraday Soc. 1, 26 (1947).

7. Lin, C. S., Denton, E. B., Gaskill, N. S., and Putnam, G. L. Ind. Eng. Chem. 45, 2136 (1951).

8. Lin, C. S., Moulton, R. W., and G. L. Putnam. Ind. Eng. Chem. 45, 636 (1953).

9. Taylor, G. I. Phil. Trans. Roy. Soc. (London) 223, 289 (1923); Proc. Roy. Soc. (London) A 151, 494 (1935).

10. Pai, Shih-I, NACA Tech. Note 892 (1943).

11. Theodorsen, T., and Regier, A. NACA Report 793 (1945).

12. Kolthoff, I. M., and Lingane, J. J. Polarography (2d ed.) Interscience, New York, 1952.

13. Tsukamoto, T., Kambara, T., and Tachi, I. J. Electrochem. Assoc. (Japan) 18, 386 (1950).

14. Brunner, E. Z. physik. Chem. 47, 56 (1904).

15. Nernst, W., and Merriam, E. S. Z. physik. Chem. 53, 235 (1905).

16. Eucken, A. Z. Elektrochem 38, 341 (1932).

17. Kambara, T., and Tsukamoto, T. J. Electrochem. Assoc. (Japan) 18, 356 (1950).

18. Raold, B., and Beak, W. J. Electrochem. Soc. 98, 277 (1951).

19. Friedenhagen, C. Z. Anorg. Chem. 29, 396 (1902).

20. Just, G. Z. physik. Chem. 63, 513 (1908).

21. Grube, G. Z. Elektrochem. 18, 189 (1912); 20, 334 (1914).

22. Moll, W. L. H. Z. physik. Chem. A 175, 353 (1936).

23. Essin, O., Derendiayer, S., and Ladygin, N. J. Applied Chem. (U.S.S.R.) 13, 971 (1940).

24. Carmody, W. R., and Rohan, J. J. Trans. Electrochem. Soc. 83, 241 (1943).

25. Petrocelli, J. V., and Paolucci, A. A. J. Electrochem. Soc. 98, 291 (1951).

26. Matuschek, J. Chem. Ztg. 25, 601 (1901).

27. Iimori, S. Z. anorg. allgem. Chem. 167, 145 (1927).

28. Kolthoff, I. M., and Pearson, E. A. Ind. Eng. Chem. Anal. Ed. 3, 381 (1931).

29. Kolthoff, I. M., and Furman, N. H. Volumetric Analysis, Vol. II, p. 427, J. Wiley and Sons, New York, 1929.

30. Sutton, F. Volumetric Analysis, 12th ed., p. 235, Blakiston Son and Co., Philadelphia, 1935.

31. Anderson, J. S., and Saddington, K. J. Chem. Soc. S381 (1949).

32. Eisenberg, M., Tobias, C. W., and Wilke, C. R. Technical Report No. 2, Nonr 222 (06).

33. Petrocelli, J. V. J. Electrochem. Soc. 98, 187 (1951).

34. Chilton, T. H., and Colburn, A. P. Ind. Eng. Chem. 26, 1183 (1934).

35. Gerischer, H. Z. Elektrochem. 54, 362 (1950); 55, 98 (1951).

36. Lewartowicz, E. J. Chimie Phys. 49, 557, 564, 573 (1952).

37. Eyring, H., Glasstone, S., and Laidler, K. J. J. Chem. Phys. 7, 1053 (1939).

38. Le Blanc, M. Abh. Bunsen Ges. No. 3 (1910).

39. Brintziger, H., and Ratanarat Ch. Z. anorg. allgem. Chem. 222, 113 (1935).

40. Sachsse, H. Z. Elektrochem. 40, 531 (1934).

41. Sutra, G. J. Chimie Physique 43, 189 (1946).

NOMENCLATURE

Symbol	Definition	Units
A	Interfacial area for mass transfer	cm^2
c_o	Concentration of reacting ions in the bulk of the solution	moles/cc
c_i	Concentration of reacting ions at the electrode interface	moles/cc
c_{ferri}	Bulk concentration of ferricyanide ions	moles/cc
c_{ferro}	Bulk concentration of ferrocyanide ions	moles/cc
d_i	Diameter of the inner rotating electrode	cm
d_o	Diameter of outside stationary electrode	cm
D_k	Diffusion coefficient of species k	cm^2/sec
ΔE_T	Total polarization	mV
ΔE_{conc}	Concentration polarization	mV
ΔE_{chem}	Chemical polarization	mV
F	Faraday equivalent 96,500	coulomb/equiv.
i_o	Exchange current density	$amps/cm^2$
I	Current density	mA/cm^2
I_a	Anodic limiting current density	mA/cm^2
I_c	Cathodic limiting current density	mA/cm^2
k	Mass transfer coefficient, generally	cm/sec
k_a	Mass transfer coefficient at the anode	cm/sec
k_c	Mass transfer coefficient at cathode	cm/sec
n	Number of electrons exchanged in the electrode reaction	
N	Rate of mass transfer	$moles/cm^2$-sec
R	Universal gas constant, 8.313×10^7	erg/°K-mole
S	Rotational speed	rpm
t	Time	sec

Nomenclature cont.

Symbol	Definition	Units
T	Temperature	°K
V	Peripheral velocity at the rotating cylinder	cm/sec
ZCP	Zero current potential (static potential difference between an investigated electrode and the reference cell)	mV

GREEK SYMBOLS

α, β	Fractions of electrical potential difference across the activation energy barrier acting in the cathodic and anodic direction respectively.	
δ	Thickness of diffusion layer	cm
$\mathcal{K}$	Electrical conductivity of a solution	$ohm^{-1}cm^{-1}$
μ	Dynamic viscosity	g/cm-sec
ν	Kinematic viscosity	cm^2/sec
ρ	Density	g/cm^3

DIMENSIONLESS GROUPS

$Q = \frac{1 \mp I/I_c}{1 \mp I/I_a}$ Ratio used in ΔE_{conc} calculations (upper sign for cathodic case, lower for anodic).

$R_d = \frac{Vd_i}{\nu}$ Reynolds number based on diameter of rotating inner cylinder.

$Sc = \frac{\nu}{D_k}$ Schmidt number for mass transfer of species k.

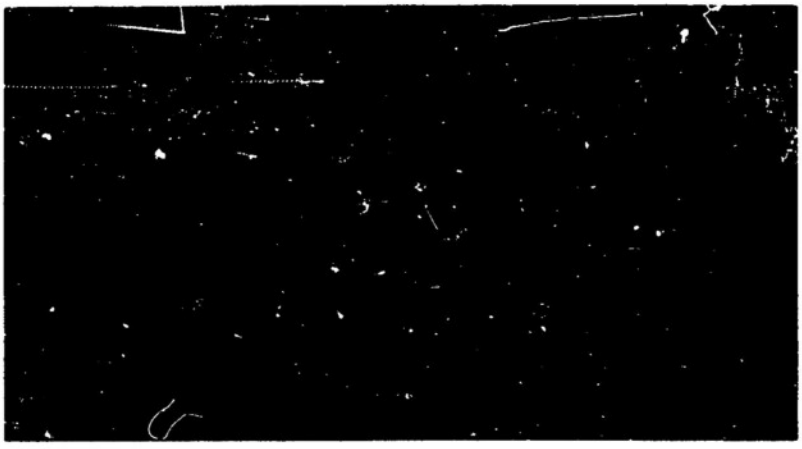

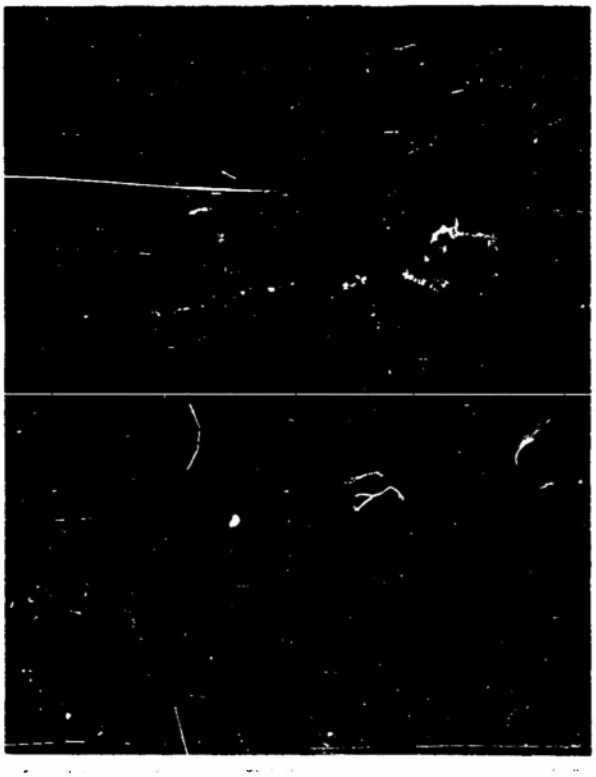

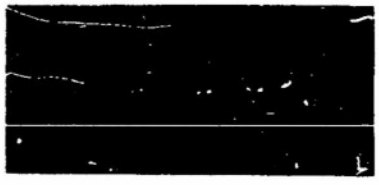

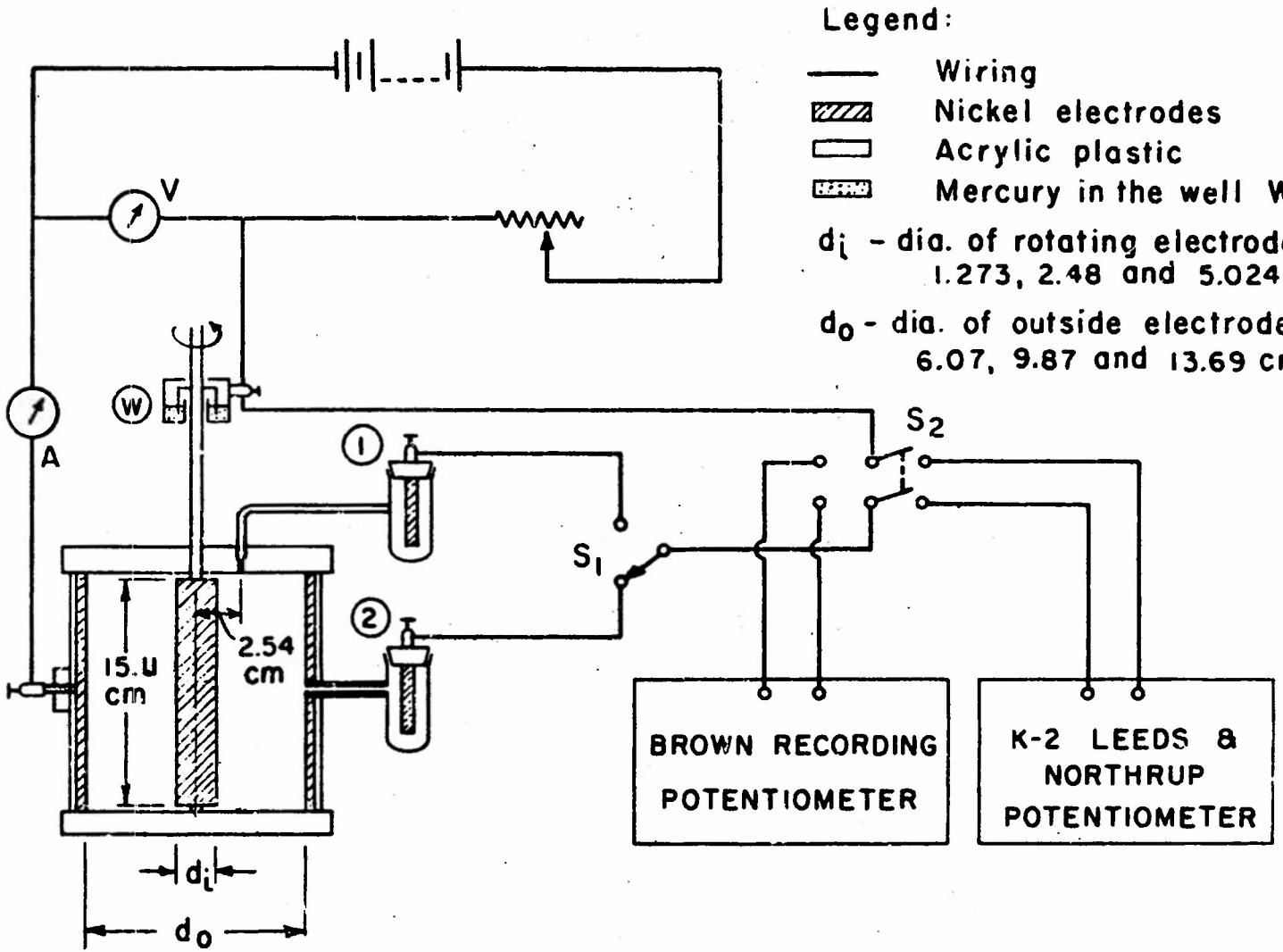

FIG. 4. SCHEMATIC DIAGRAM OF THE ELECROLYSING AND MEASURING CIRCUITS USED WITH THE CELL FOR ROTATING ELECTRODES.

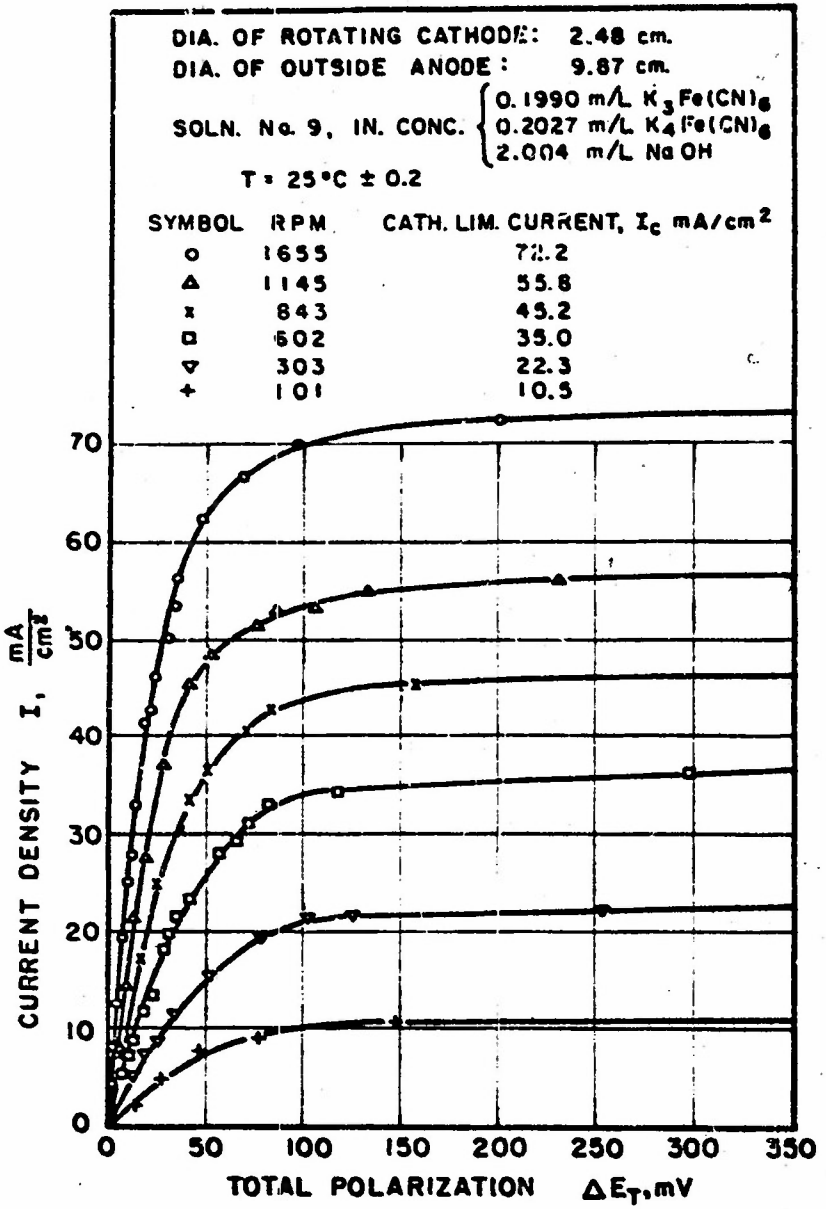

FIG. 5 CATHODIC POLARIZATION CURVES OF FERRICYANIDE ION REDUCTION

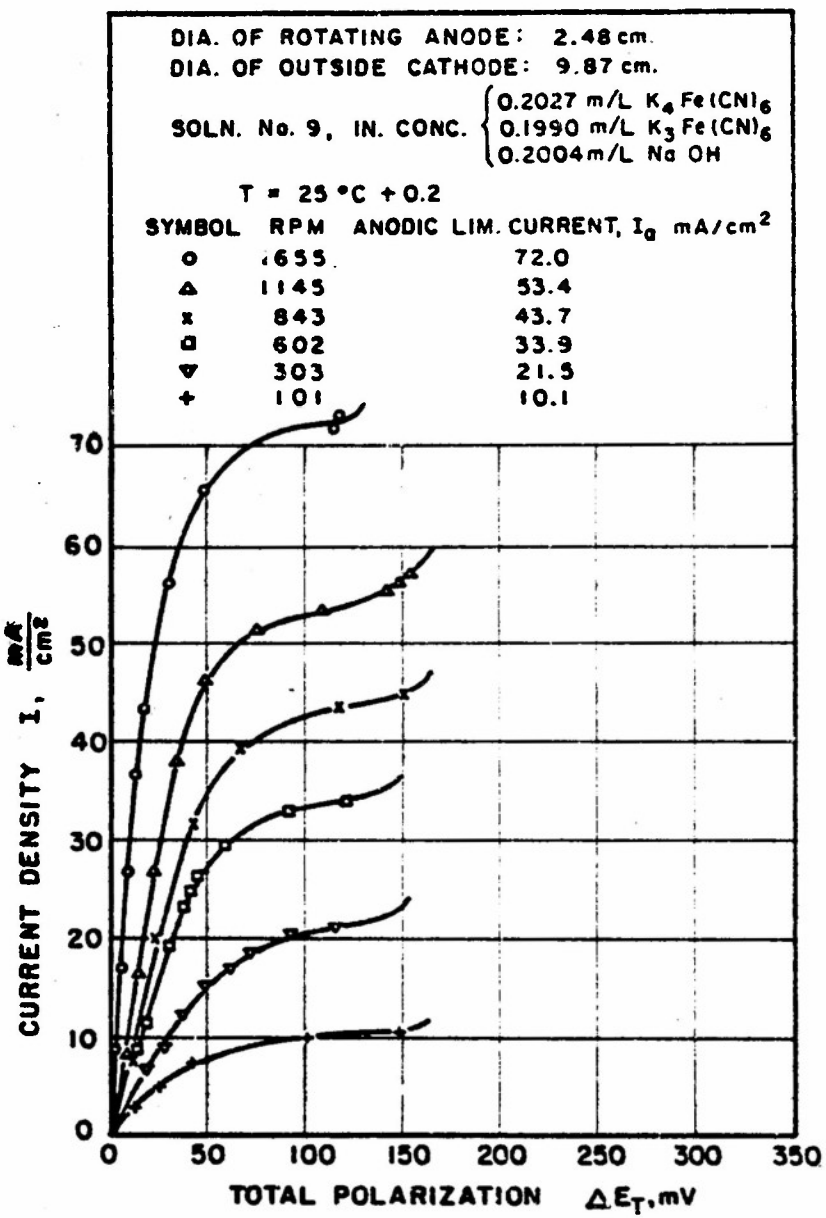

FIG. 6 ANODIC POLARIZATION CURVES OF FERROCYANIDE ION OXIDATION

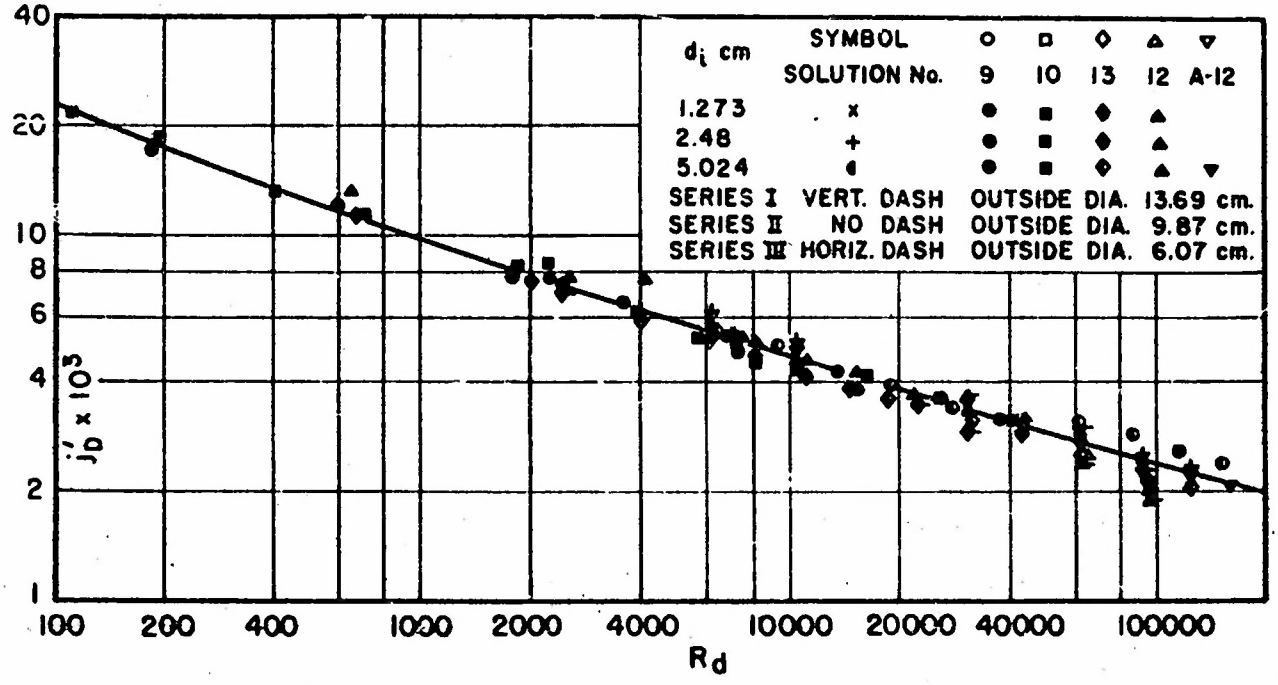

FIG. 7 CATHODIC REDUCTION OF FERRICYANIDE
MASS TRANSFER AT ROTATING ELECTRODES
$j'_D = \frac{k_c}{V}(Sc)^{0.644}$ vs R_d

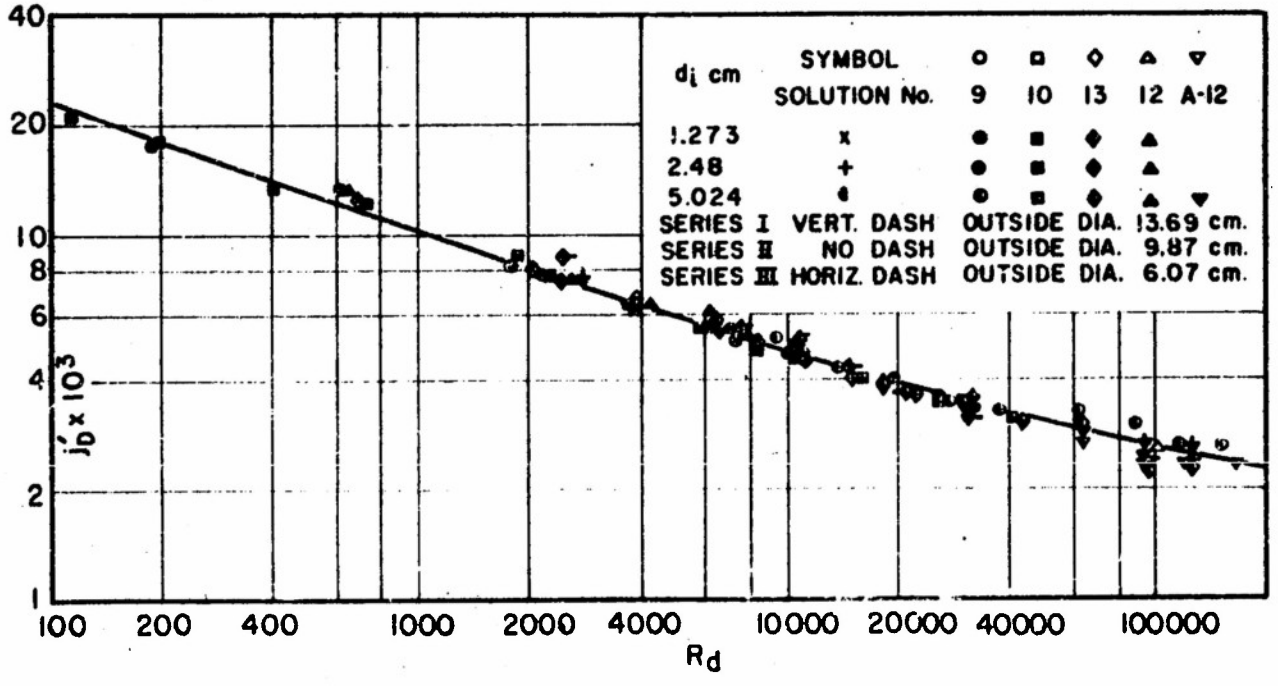

FIG. 8 ANODIC OXIDATION OF FERROCYANIDE
MASS TRANSFER AT ROTATING ELECTRODES
$j'_D = \frac{k_g}{V}(Sc)^{0.644}$ vs R_d

Contract Personnel

Morris Eisenberg	, Research Engineer
A. Hardt	, Laboratory Assistant
J. Worley	, Laboratory Assistant
L. Wolf	, Laboratory Assistant
Charles W. Tobias	, Project Co-director
Charles R. Wilke	, Project Co-director

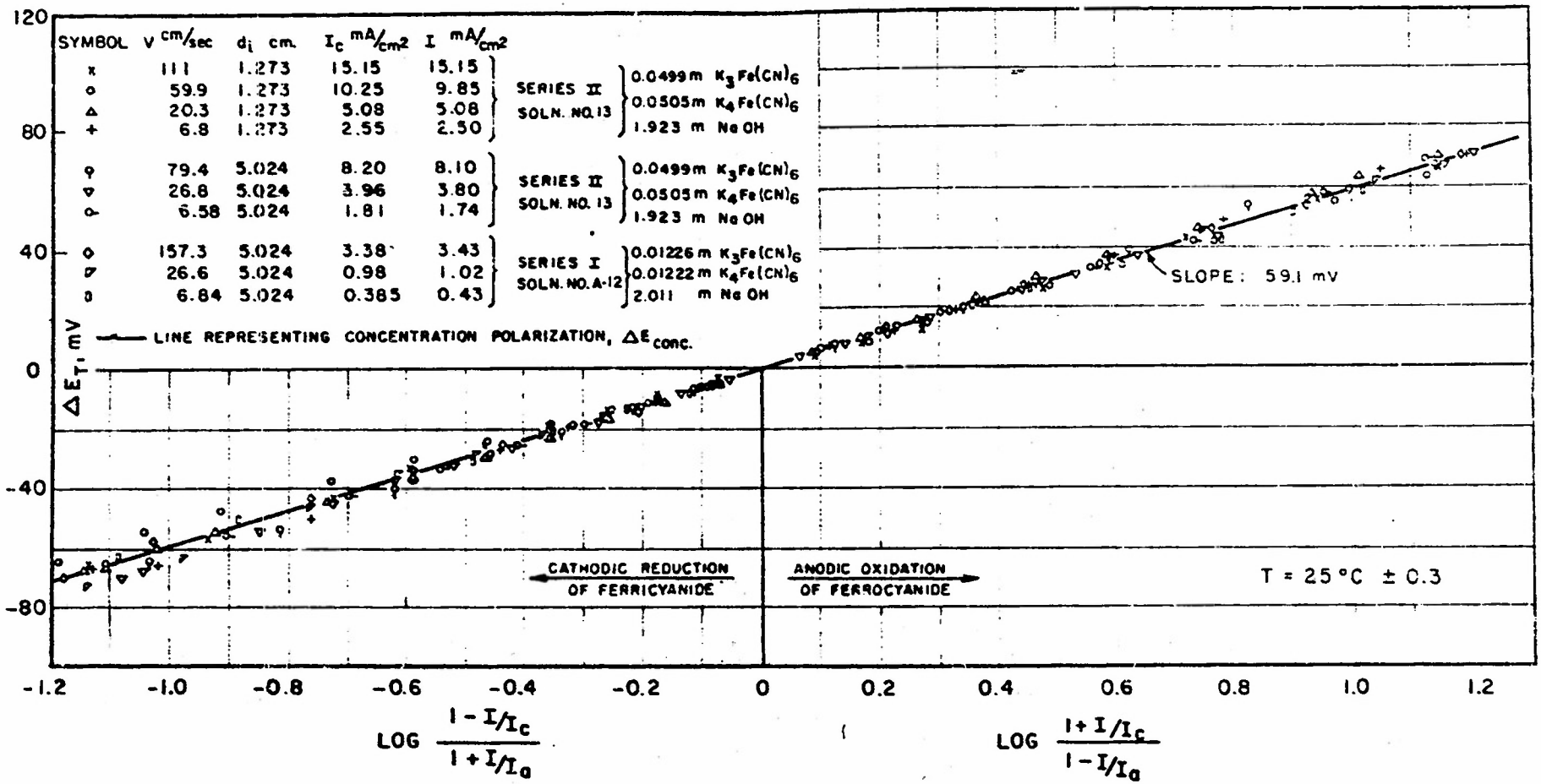

FIG. 11 TOTAL POLARIZATION ΔE_T vs LOG Q

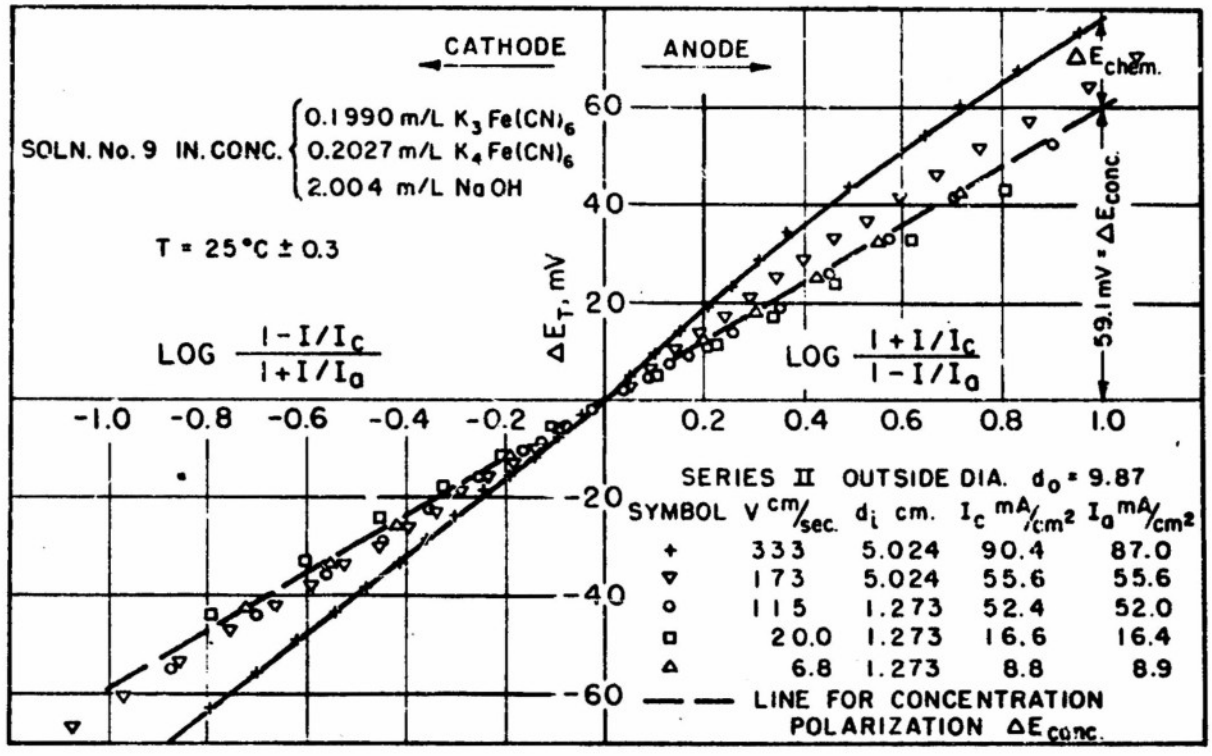

FIG. 12 TOTAL POLARIZATION ΔE_T vs LOG Q FOR HIGH CURRENT DENSITY ELECTROLYSIS

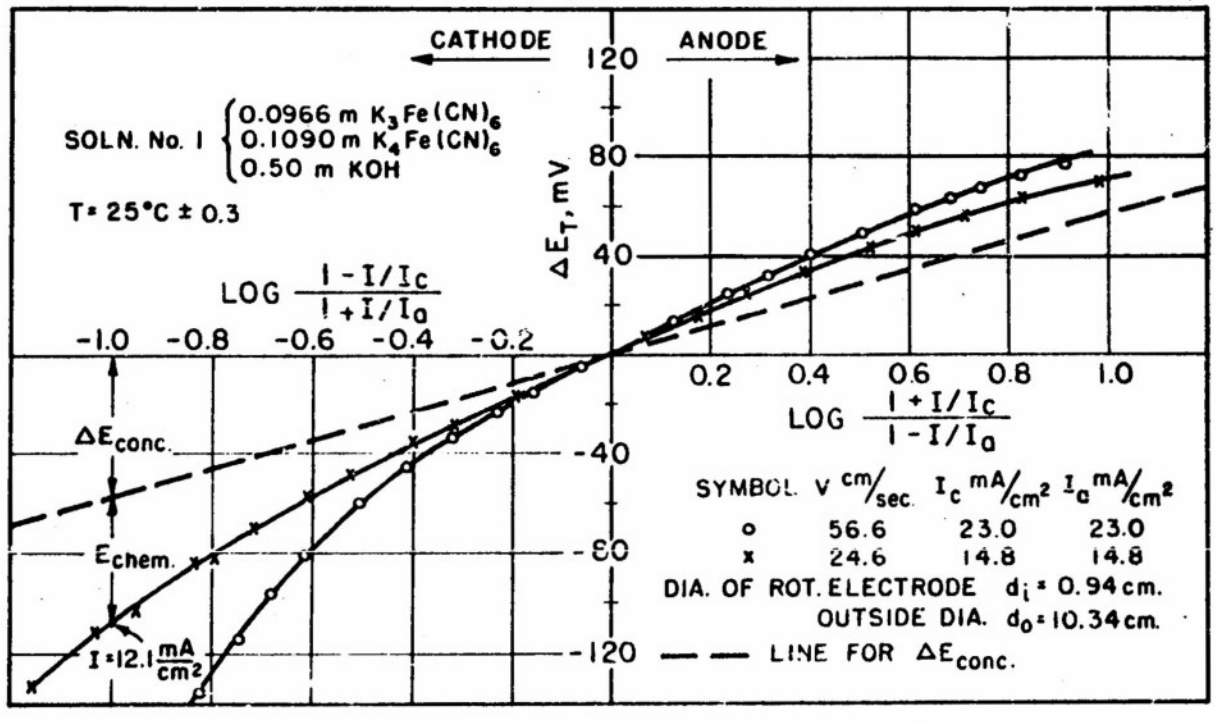

FIG 13 TOTAL POLARIZATION ΔE_T vs LOG Q IN CASE OF "INACTIVE ELECTRODES" AND PRESENCE OF AIR-OXYGEN

Table I. Mass Transfer at Rotating Electrodes, Ferri-Ferrocyanide Couple.

Solution No. 9, (2.004 N NaOH)

Run No.	V cm/sec	T °C	$\nu \times 10^2$ cm²/sec	R_d	Cathodic Reduction of Ferricyanide: $C_{ferri} \times 10^3$ mol/cc	I_c mA/cm²	$k_c \times 10^5$ cm/sec	$D \times 10^5$ cm²/sec	Sc	$j'_D \times 10^3$	Anodic Oxidation of Ferrocyanide: $C_{ferro} \times 10^3$ mol/cc	I_a mA/cm²	$k_a \times 10^5$ cm/sec	$D \times 10^5$ cm²/sec	Sc	$j'_D \times 10^3$
13a, d_i = 1.273 cm., A = 61.2 cm² Ser. II (d_o = 9.87 cm)																
-,276A	114.9	25	1.423	10,280	-	-	-	-	-	-	0.2030	52.0	263.5	0.390	3,649	4.55
277C,278A	81.5	"	"	7,291	0.1988	42.2	218.8	0.454	3,134	4.82	0.2029	42.0	214.4	"	"	5.18
280C,281A	40.4	"	"	3,614	0.1982	28.2	147.3	"	"	6.51	0.2028	28.0	132.6	"	"	6.46
284C,285A	20.0	"	"	1,789	0.1976	16.6	87.0	"	"	7.76	0.2027	16.4	83.9	"	"	8.27
286C,287A	6.8	"	"	608	0.1971	8.8	46.2	"	"	12.1	0.2026	8.9	45.4	"	"	13.1
290C,291A	2.07	"	"	185	0.1961	3.76	19.9	"	"	17.1	0.2024	3.55	18.2	"	"	17.3
13b, d_i = 2.48 cm. A = 117.6 cm² Ser. II (d_o = 9.87 cm)																
133C, 134A	214.9	25	1.423	37,460	0.1990	72.2	376	0.454	3,134	3.12	0.2027	72.0	368	0.390	3,649	3.37
135C,136A	148.7	"	"	25,920	0.1970	55.8	294	"	"	3.53	0.2026	53.4	273	"	"	3.62
137C,138A	109.5	"	"	19,080	0.1960	45.2	239	"	"	3.89	0.2025	43.7	224	"	"	4.03
139C, 140A	78.2	"	"	13,630	0.1945	35.0	186	"	"	4.25	0.2024	33.9	174	"	"	4.37
141C,142A	39.3	"	"	6,850	0.1935	22.3	119	"	"	5.41	0.2023	21.5	110.1	"	"	5.51
145C,144A	13.1	"	"	2,283	0.1928	10.8	57	"	"	7.76	0.2023	10.1	51.8	"	"	7.77
13c, d_i = 5.024 cm A = 236.4 cm² Ser. II, (d_o = 9.87 cm)																
484C, 485A	26.6	25	1.423	9,361	0.1961	13.60	74.5	0.454	3,134	5.00	0.2030	13.80	70.4	0.390	3,649	5.22
486C, 487A	78.7	"	"	28,140	0.1964	27.8	151.3	"	"	3.39	0.2037	27.40	139.4	"	"	3.44
488C, 489A	172.6	"	"	61,010	0.1938	56.6	300.3	"	"	3.11	0.2044	55.6	281.9	"	"	3.21
490C, 491A	246.2	"	"	87,130	0.1930	73.3	393.8	"	"	2.84	0.2050	75.0	379.1	"	"	3.03
492C, 493A	332.2	"	"	117,500	0.1969	90.4	475.9	"	"	2.55	0.2024	87.0	445.4	"	"	2.64
494C, 495A	426.2	25.7	1.406	152,400	0.1963	109.0	575.6	0.461	3,048	2.57	0.2024	115.0	578.6	0.396	3,548	2.63

$$R_d = \frac{Vd_i}{\nu} \qquad j'_D = \frac{k}{V}(Sc)^{0.644}$$

Table 2

Coordinates of the General Mass Transfer Correlation Curve for Rotating Cylinders (see Fig. 10).

R_d	$j_D' \times 10^3$
200	18.4
500	13.0
1,000	10.2
4,000	6.53
10,000	4.88
30,000	3.54
60,000	2.96
100,000	2.61
200,000	2.24
300,000	2.05

Table 3

Concentration and Chemical Polarizations
at Various Rotational Speeds
and Current Densities

Solution No. 13, Series II.

Initial composition : (0.04996 m/L $K_3Fe(CN)_6$
(0.05052 m/L $K_4Fe(CN)_6$
(1.923 m/L NaOH

T = 25.0°C.
Rotor diameter (d_i) = 5.024 cm.
Outer cylinder diameter (d_o) = 9.87 cm.

Run No.	I mA/cm²	Cathodic Reduction of $Fe(CN)_6^{-3}$			Anodic Oxidation of $Fe(CN)_6^{-4}$		
		$\Delta E^*_{conc.}$ (calc.) mV	ΔE_T (meas.) mV	$\Delta E_{chem} = \Delta E_T - \Delta E_{conc.}$ mV	$\Delta E^*_{conc.}$ (calc.) mV	ΔE_T (meas.) mV	$\Delta E_{chem} = \Delta E_T - \Delta E_{conc.}$ mV
		1208 rpm; V = 318 cm/sec. I_c = 22.00 mA/cm²; I_a = 21.00 mA/cm².					
15a	2	-4.5	-4.0	0.5	4.8	4.C	-0.8
	4	-9.6	-9.1	0.5	9.7	8.1	-1.6
	6	-14.6	-12.4	2.2	14.8	12.4	-2.4
	8	-19.9	-17.2	2.7	20.3	17.2	-3.1
	10	-25.6	-21.6	4.0	26.3	21.6	-4.7
	12	-31.9	-26.7	5.2	33.0	27.8	-5.2
	14	-39.1	-34.1	5.0	40.8	36.3	-4.5
	16	-47.9	-43.0	4.9	50.9	50.0	-0.9
	18	-59.8	-56.7	3.1	65.5	67.2	1.7
	18.5	-63.6	-61.6	2.0	70.5	72.8	2.3
		302 rpm; V = 79.4 cm/sec. I_c = 8.20 mA/cm²; I_a = 8.10 mA/cm²					
15b	1.	-6.3	-6.4	-0.1	6.3	6.4	0.1
	2	-12.8	-13.0	-0.2	12.9	13.0	0.1
	3	-19.7	-20.3	-0.6	19.8	20.3	0.5
	4	-27.5	-28.9	-1.4	27.7	28.9	1.2
	5	-36.5	-39.7	-3.2	36.9	39.7	2.8
	6	-48.1	-53.9	-5.8	48.8	53.9	5.1
		102 rpm; V = 26.8 cm/sec. I_c = 3.96 mA/cm²; I_a = 3.80 mA/cm²					
15c	0.3	-4.0	-4.0	0.0	4.0	4.0	0.0
	0.6	-8.0	-7.9	0.1	8.0	7.9	-0.1
	0.9	-12.1	-12.1	0.0	12.2	12.1	-0.1
	1.2	-16.3	-16.7	-0.4	16.6	16.7	0.1
	1.5	-20.8	-20.9	-0.1	21.1	20.9	-0.2
	1.8	-25.5	-26.0	-0.5	26.1	26.0	-0.1
	2.1	-30.7	-31.2	-0.5	31.6	31.2	-0.4
	2.4	-36.6	-37.1	-0.5	37.9	37.1	-0.8
	2.7	-43.3	-44.2	-0.9	45.2	44.2	-1.0
	3.0	-51.4	-54.2	-2.8	54.5	54.2	-0.3
	3.3	-62.1	-68.0	-5.9	67.7	68.0	0.3
	3.36	-64.8	-71.0	-6.2	71.3	71.0	-0.3
		25 rpm; V = 6.58 cm/sec. I_c = 1.81 mA/cm²; I_a = 1.74 mA/cm²					
15d	0.2	-5.8	-6.2	-0.4	5.8	6.2	0.4
	0.4	-11.7	-12.1	-0.4	11.8	12.1	0.3
	0.6	-17.8	-18.5	-0.7	17.8	18.5	0.7
	0.8	-24.7	-25.3	-0.6	25.2	25.3	0.1
	1.0	-32.3	-33.0	-0.7	33.3	33.0	-0.3
	1.2	-41.4	-42.6	-1.2	43.1	42.6	-0.5
	1.4	-53.3	-55.2	-1.9	56.7	57.0	-0.3
	1.5	-61.2	-64.7	-3.5	66.3	68.7	2.4

* $\Delta E_{conc}(mV) = 59.1 \text{ Log } \frac{1 \mp I/I_c}{1 \pm I/I_a}$

(Upper sign for cathodic case, lower for anodic.)

Table 4

Concentration and Chemical Polarizations at Various Rotational Speeds and Current Densities

Solution No. A-12, Series I

Initial composition: (0.01118 m/L $K_3Fe(CN)_6$
(0.01424 m/L $K_4Fe(CN)_6$
(2.011 m/L NaOH

T = 25.0°C.
Rotor diameter (d_i) = 5.024 cm.
Outer cylinder diameter (d_o) = 13.69 cm.

Run No.	I mA/cm²	Cathodic Reduction of $Fe(CN)_6^{-3}$			Anodic Oxidation of $Fe(CN)_6^{-4}$		
		$\Delta E_{conc.}$ (calc.) mV	ΔE_T (meas.) mV	$\Delta E_{chem.} = \Delta E_T - \Delta E_{conc.}$ mV	$\Delta E_{conc.}$ (calc.) mV	ΔE_T (meas.) mV	$\Delta E_{chem.} = \Delta E_T - \Delta E_{conc.}$ mV
		1225 rpm; V = 322.24 cm/sec. I_c = 5.88 mA/cm²; I_a = 5.91 mA/cm².					
16a	0.6	-5.4	-5.2	0.2	4.8	5.2	0.4
	1.2	-9.1	-10.7	-1.6	11.0	11.2	0.2
	1.8	-16.5	-16.1	0.4	16.8	17.5	0.7
	2.4	-22.6	-21.8	0.8	23.2	23.2	0.0
	3.0	-29.4	-27.9	1.5	30.4	30.0	-0.4
	3.6	-37.1	-35.8	1.3	38.8	38.1	-0.7
	4.2	-46.5	-46.5	0.0	49.6	49.9	0.3
	4.8	-58.8	-61.5	-2.7	58.0	66.1	6.1
	5.1	-67.8	-71.0	-3.2	66.9	76.6	9.7
		598 rpm; V = 157.31 cm/sec. I_c = 3.38 mA/cm²; I_a = 3.43 mA/cm².					
16b	0.4	-6.1	-6.2	-0.1	6.1	6.2	0.1
	0.8	-12.3	-12.5	-0.2	12.2	12.5	0.3
	1.2	-19.0	-19.1	-0.1	18.9	19.1	0.2
	1.6	-26.3	-26.3	0.0	26.1	26.3	0.2
	2.0	-34.8	-34.3	0.5	34.4	34.9	0.5
	2.4	-45.4	-43.9	1.5	44.8	45.3	0.5
	2.8	-60.3	-58.3	2.0	59.1	59.2	0.1
	3.0	-70.1	-70.0	0.1	69.9	70.0	0.1
		101 rpm; V = 26.569 cm/sec. I_c = 0.98 mA/cm²; I_a = 1.02 mA/cm².					
16c	0.1	-5.2	-5.0	0.2	5.1	5.0	0.1
	0.2	-10.4	-10.2	0.2	10.4	10.2	-0.2
	0.3	-16.0	-15.7	0.3	15.8	15.7	-0.1
	0.4	-21.9	-21.7	0.2	21.6	21.7	0.1
	0.5	-28.5	-28.2	0.3	27.9	28.2	0.3
	0.6	-36.2	-36.0	0.2	35.0	36.0	1.0
	0.7	-45.5	-46.5	-1.0	43.6	44.8	1.2
	0.8	-58.3	-62.0	-3.7	54.6	55.7	1.1
	0.85	-67.4	-72.5	-5.1	61.8	62.1	0.3
		26 rpm; V = 6.8395 cm/sec. I_c = 0.385 mA/cm²; I_a = 0.430 mA/cm².					
16d	0.05	-6.4	-6.7	-0.3	6.3	5.5	-0.8
	0.10	-13.1	-13.7	-0.6	12.7	12.2	-0.5
	0.15	-20.4	-20.5	-0.1	19.4	18.8	-0.6
	0.20	-28.6	-29.1	-0.5	26.8	26.6	-0.2
	0.25	-38.7	-38.5	0.1	35.2	35.5	+0.3
	0.30	-52.3	-51.0	1.3	45.4	44.8	-0.6
	0.33	-64.5	-62.7	1.8	53.4	51.0	-2.4
	0.35	-	-	-	59.9	57.1	-2.8

Table 5

Concentration and Chemical Polarizations at Various Rotational Speeds and Current Densities

Solution No. 9, Series II

Initial composition: (0.1994 m /L $K_3Fe(CN)_6$
(0.2030 m/L $K_4Fe(CN)_6$
(2.004 m/L NaOH

T = 25.0°C.
Rotor diameter (d_i) = 1.273 cm.
Outer cylinder diameter (d_o) = 9.87 cm.

Run No.	I mA/cm²	Cathodic Reduction of $Fe(CN)_6^{-3}$			Anodic Oxidation of $Fe(CN)_6^{-4}$		
		$\Delta E_{conc.}$ (calc.) mV	ΔE_T (meas.) mV	$\Delta E_{chem.} = \Delta E_T - \Delta E_{conc.}$ mV	$\Delta E_{conc.}$ (calc.) mV	ΔE_T (meas.) mV	$\Delta E_{chem.} = \Delta E_T - \Delta E_{conc.}$ mV
		1724 rpm; V = 115 cm/sec. I_c = 52.4 mA/cm²; I_a = 52.0 mA/cm².					
17a	2	-2.0	-2.6	-0.6	2.00	1.9	-0.1
	5	-4.9	-5.5	-0.6	5.0	4.3	-0.7
	8	-7.9	-8.4	-0.5	7.9	7.1	-0.8
	10	-10.0	-10.4	-0.4	9.97	9.0	-1.0
	12	-12.0	-12.5	-0.5	12.03	11.0	-1.0
	15	-15.2	-15.8	-0.6	15.2	13.9	-1.3
	20	-20.7	-22.0	-1.3	20.8	19.2	-1.6
	25	-26.7	-28.6	-1.9	26.9	26.0	-0.9
	30	-33.5	-35.9	-2.4	33.7	33.0	-0.7
	35	-41.6	-44.0	-2.4	41.9	41.6	-0.3
	40	-51.8	-54.2	-2.4	53.4	52.6	-0.8
	45	-66.5	-68.5	-2.0	67.5	66.7	-0.8
		300 rpm; V = 20.0 cm/sec. I_c = 16.6 mA/cm²; I_a = 16.4 mA/cm².					
17b	2	-6.25	-5.6	0.6	6.3	5.6	-0.7
	4	-12.68	-11.5	1.2	11.5	11.5	0.0
	6	-19.50	-17.7	1.8	19.6	17.7	-1.9
	8	-27.1	-24.5	2.6	27.3	24.5	-2.8
	10	-35.9	-33.0	2.9	36.3	32.8	-3.5
	12	-47.1	-43.5	3.6	47.8	43.6	-4.2
	14	-63.5	-59.7	3.8	64.9	59.7	-5.2
	14.5	-69.4	-66.0	3.4	71.4	66.0	-5.4
		102 rpm; V = 6.80 cm/sec. I_c = 8.8 mA/cm²; I_a = 8.9 mA/cm².					
17c	1	-5.8	-5.7	0.1	5.8	5.8	0.0
	2	-11.8	-11.9	-0.1	11.7	11.8	0.1
	3	-18.2	-18.4	-0.2	18.06	18.2	0.1
	4	-25.1	-25.6	-0.5	25.0	25.6	0.6
	5	-33.0	-33.1	-0.1	32.7	33.3	0.6
	6	-42.7	-42.6	0.1	42.2	42.5	0.3
	7	-55.7	-54.4	1.3	54.7	54.4	-0.3
	7.5	-64.9	-64.0	0.9	63.6	62.0	-1.6
	8	-77.6	-76.2	1.4	75.4	73.2	-2.2

Table 6

Concentration and Chemical Polarizations at Various Rotational Speeds and Current Densities

Solution No. 9, Series II

Initial composition: (0.1994 m/L $K_3Fe(CN)_6$
(0.2030 m/L $K_4Fe(CN)_6$
(2.004 m/L NaOH

$T = 25^{\circ}C$.
Rotor diameter (d_i) = 5.024 cm.
Outer cylinder diameter (d_o) = 9.87 cm.

Run No.	I	Cathodic Reduction of $Fe(CN)_6^{-3}$			Anodic Oxidation of $Fe(CN)_6^{-4}$		
		$\Delta E_{conc.}$ (calc.)	ΔE_T (meas.)	$\Delta E_{chem.} = \Delta E_T - \Delta E_{conc.}$	$\Delta E_{conc.}$ (calc.)	ΔE_T (meas.)	$\Delta E_{chem.} = \Delta E_T - \Delta E_{conc.}$
	mA/cm^2	mV	mV	mV	mV	mV	mV
		1265 rpm; V = 333 cm/sec. I_c = 90.4 mA/cm^2; I_a = 87.0 mA/cm^2.					
18a	5	-2.9	-3.1	-0.2	2.9	4.9	2.0
	10	-5.7	-7.5	-1.8	5.7	9.8	4.1
	15	-8.7	-11.5	-2.8	8.8	14.6	5.8
	20	-11.7	-15.5	-3.8	12.2	19.2	7.0
	25	-14.8	-18.6	-3.8	15.0	23.1	8.1
	30	-18.0	-23.6	-5.6	18.2	28.9	10.7
	35	-21.3	-28.0	-6.7	21.7	34.7	13.0
	40	-24.7	-33.2	-8.5	25.2	38.3	13.7
	45	-28.5	-38.0	-9.5	29.1	43.2	14.1
	50	-32.3	-43.1	-10.8	33.3	48.7	15.4
	55	-36.7	-48.7	-12.0	37.9	54.3	16.4
	60	-41.4	-55.1	-13.7	42.3	60.4	18.1
	65	-47.0	-62.3	-15.3	49.2	67.4	18.2
	70	-53.5	-70.8	-17.3	56.7	75.0	18.3
	75	-61.5	-81.8	-20.3	66.5	83.5	17.0
	77	-65.4	-87.3	-21.9	71.3	88.3	17.0
		657 rpm; V = 173 cm/sec. I_c = 55.6 mA/cm^2; I_a = 55.6 mA/cm^2					
18b	3	-2.8	-3.0	-0.2	2.8	3.3	0.5
	6	-5.6	-5.9	-0.3	5.6	6.8	1.2
	9	-8.4	-9.2	-0.8	8.4	10.2	1.8
	12	-11.3	-12.3	-1.0	11.3	13.9	2.6
	15	-14.2	-15.3	-1.1	14.2	17.5	3.3
	18	-17.3	-18.6	-1.3	17.2	21.1	3.9
	21	-20.4	-22.0	-1.6	20.4	25.0	4.6
	24	-23.7	-25.7	-2.0	23.7	29.0	5.3
	27	-27.2	-29.3	-2.1	27.2	33.1	5.9
	30	-31.0	-33.2	-2.2	31.0	37.1	6.1
	33	-35.0	-37.4	-2.4	35.0	41.7	6.7
	36	-39.5	-41.7	-2.2	39.5	46.1	6.6
	39	-44.6	-46.8	-2.2	44.6	51.3	6.7
	42	-50.6	-53.0	-2.4	50.7	57.3	6.6
	45	-57.6	-60.0	-2.4	57.6	64.4	6.8
	47	-63.6	-66.1	-2.5	63.6	70.0	6.4